Supporting information for:

"Towards an optimal metal for CNTFETs"

Artem Fediai,[*,†,‡] Dmitry A. Ryndyk,[†,‡] Gotthard Seifert,[¶,‡,§] Sven Mothes,[‖,‡]

Martin Claus,[‖,‡] Michael Schröter,[‖,‡] and Gianaurelio Cuniberti[†,‡,§]

†*Institute for Materials Science and Max Bergmann Center of Biomaterials, TU Dresden, 01062 Dresden, Germany*

‡*Center for Advancing Electronics Dresden, TU Dresden, 01062 Dresden, Germany*

¶*Theoretical Chemistry, TU Dresden, 01062 Dresden, Germany*

§*Dresden Center for Computational Materials Science (DCMS), TU Dresden, 01062 Dresden, Germany*

‖*Department of Electrical and Computer Engineering, TU Dresden, 01062 Dresden, Germany*

E-mail: artem.fediai@nano.tu-dresden.de

Physical characteristics of the CNT-metal contacts for each of the metals

Figures S1 to S10 provide comprehensive and convenient information on each of 10 CNT-metal contacts, including: (a) spectral function $A(k, E)$; (b) density of states in the embedded tube portion projected onto carbon atom $\text{DOS}_{\text{inside}}(E)$; (c) density of states along the tube of 9-nm channel CNTFET, including ≈ 2 nm of the embedded tube on each side $\text{DOS}(z, E)$; (d) zero-bias transmission coefficient for 40-nm channel CNTFET $T(E)$.
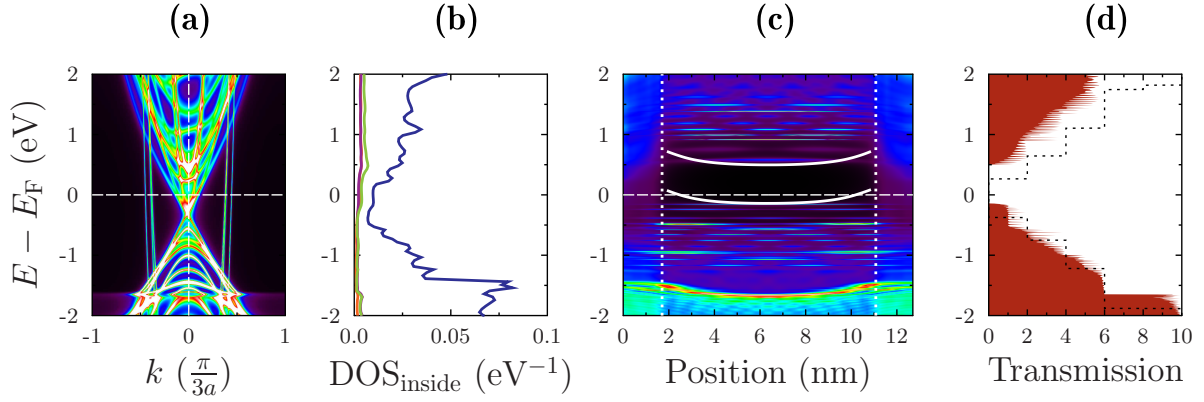
(a) **(b)** **(c)** **(d)**

Figure S1: Au-CNT contact: **(a)** $A(k, E)$, **(b)** DOS_{inside}, **(c)** $DOS(z, E)$, **(d)** $T(E)$.

(a) **(b)** **(c)** **(d)**
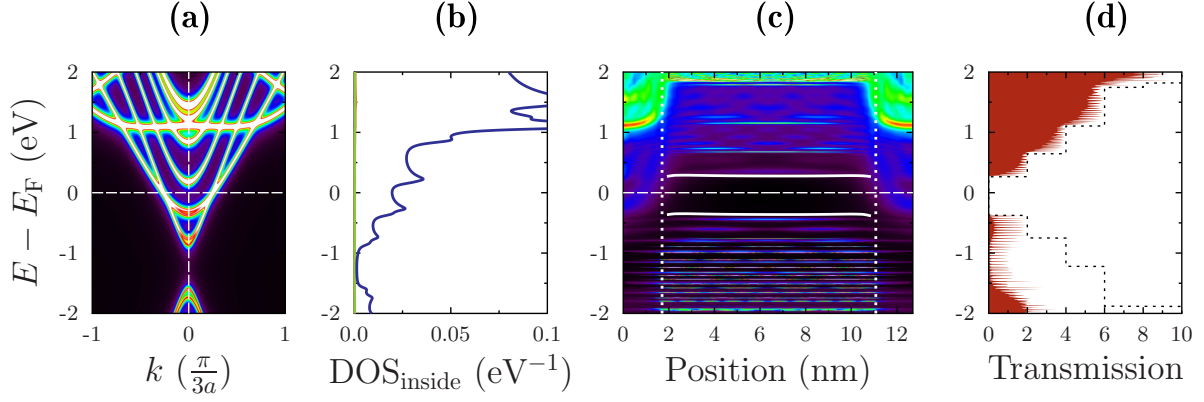
Figure S2: Al-CNT contact: **(a)** $A(k, E)$, **(b)** DOS_{inside}, **(c)** $DOS(z, E)$, **(d)** $T(E)$.

(a) **(b)** **(c)** **(d)**
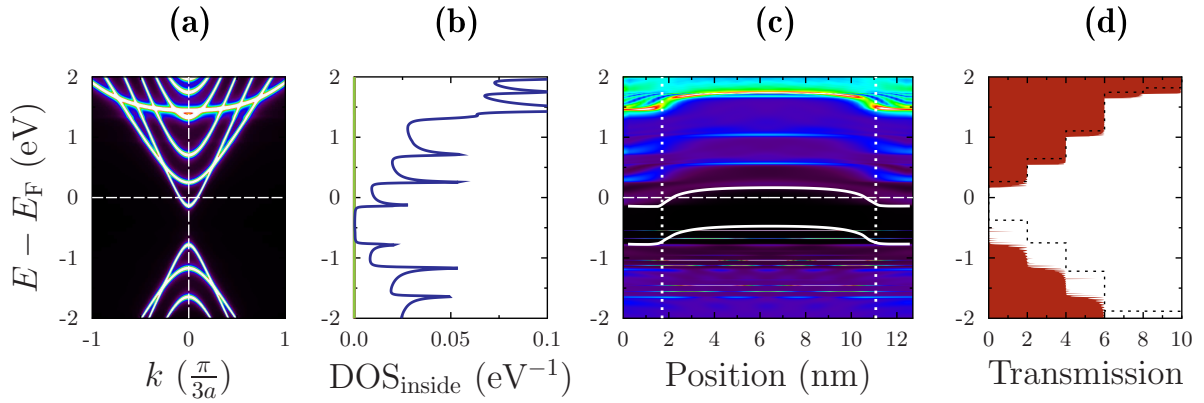
Figure S3: Cr-CNT contact: **(a)** $A(k, E)$, **(b)** DOS_{inside}, **(c)** $DOS(z, E)$, **(d)** $T(E)$.
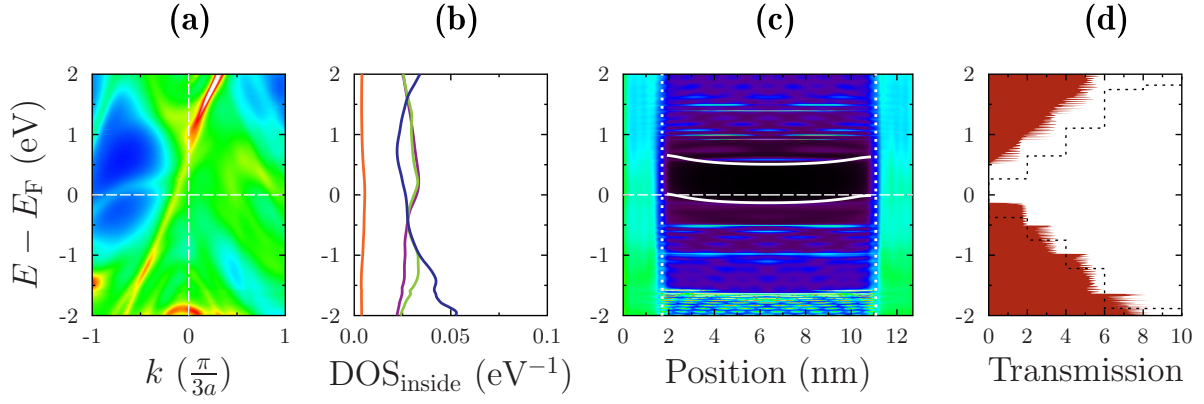
Figure S4: Cu-CNT contact: **(a)** $A(k, E)$, **(b)** DOS_{inside}, **(c)** $DOS(z, E)$, **(d)** $T(E)$.
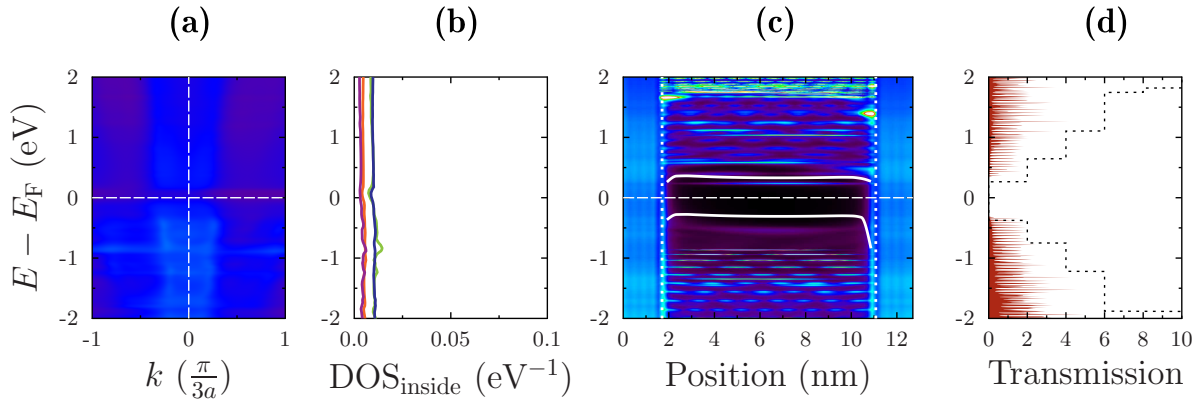
Figure S5: Ni-CNT contact: **(a)** $A(k, E)$, **(b)** DOS_{inside}, **(c)** $DOS(z, E)$, **(d)** $T(E)$.
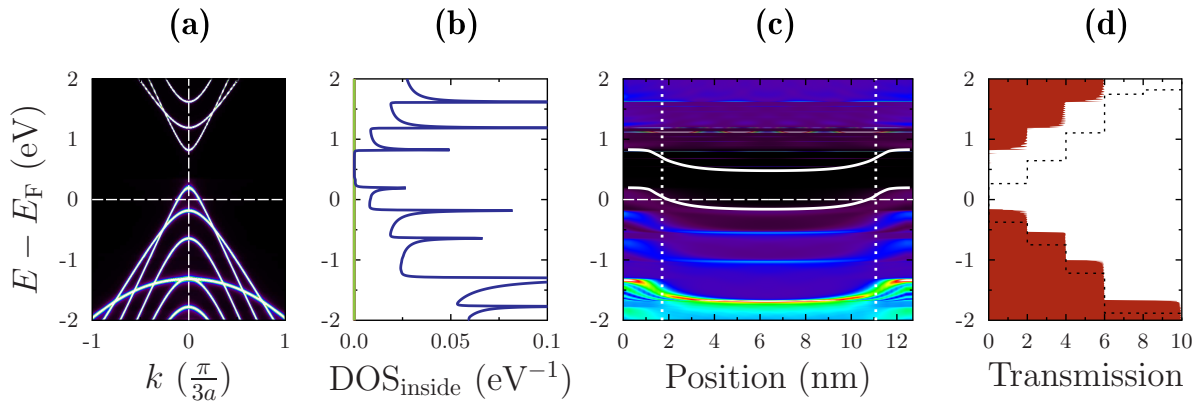
Figure S6: Pd-CNT contact: **(a)** $A(k, E)$, **(b)** DOS_{inside}, **(c)** $DOS(z, E)$, **(d)** $T(E)$.
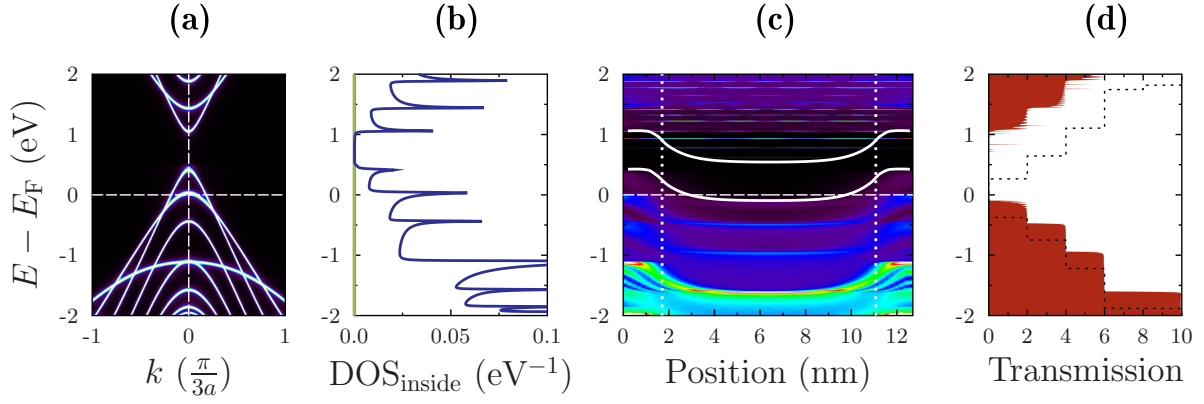
Figure S7: Pt-CNT contact: **(a)** $A(k, E)$, **(b)** DOS_{inside}, **(c)** $DOS(z, E)$, **(d)** $T(E)$.
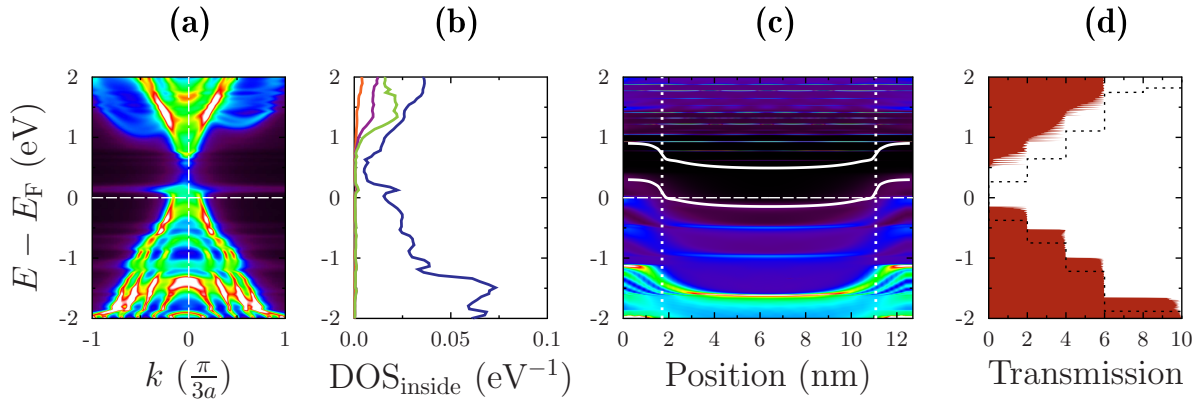
Figure S8: Rh-CNT contact: **(a)** $A(k, E)$, **(b)** DOS_{inside}, **(c)** $DOS(z, E)$, **(d)** $T(E)$.
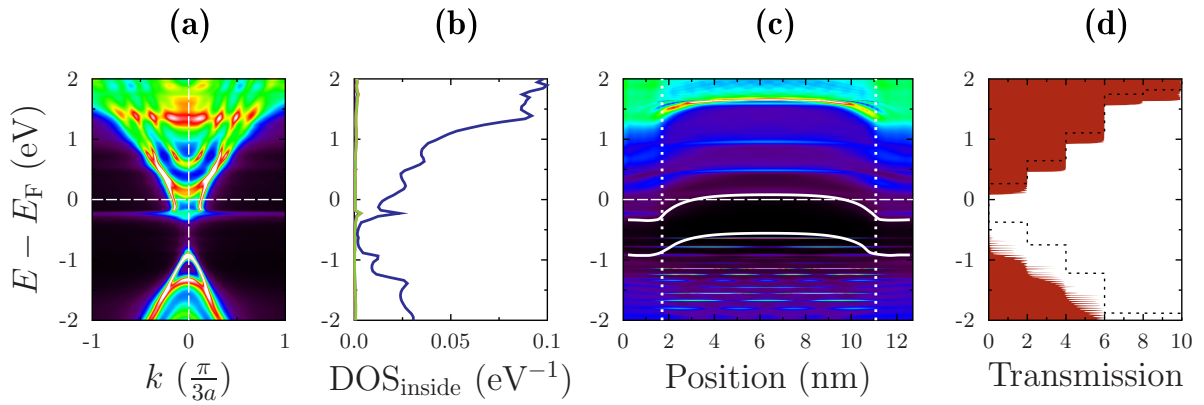
Figure S9: Sc-CNT contact: **(a)** $A(k, E)$, **(b)** DOS_{inside}, **(c)** $DOS(z, E)$, **(d)** $T(E)$.
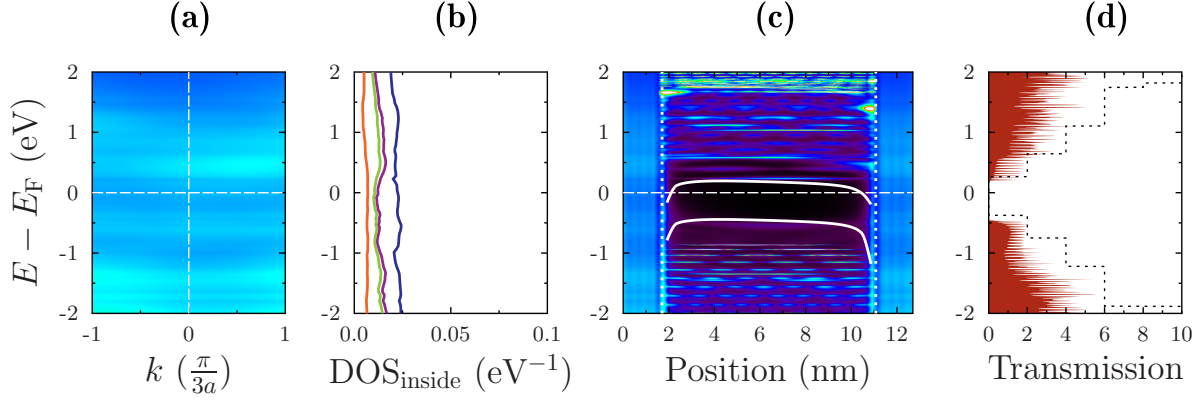
Figure S10: Ti-CNT contact: **(a)** $A(k, E)$, **(b)** $\mathrm{DOS_{inside}}$, **(c)** $\mathrm{DOS}(z, E)$, **(d)** $T(E)$.

Geometry of the simulated systems

Our special NEGF+DFT approach adapted for extended contacts implies simulation of the three systems:

1. *System* 1. Thirty periods of the "rolled-out" (16,0) CNT by its ends lying on the metal (arrangement of metal's atoms depends on type of the crystalline lattice and lattice constants. Within the contact, metal and carbon could be represented of the supercells with a common transverse period). Circular boundary conditions are applied in all spatial directions, in vertical direction we add 10 nm of vacuum. What do we take out of this system? – We take matrix Hamiltonian of the carbon subsystem **H** in a tight-binding form. To get matrix elements of the arbitrarily long contacts, we "elongate" side elements of the **H** by repeating its edge elements ($\epsilon_{1(30)}$, $t_{1(30)}$). To get a Hamiltonian, which correspondent to arbitrarily long CNT channel we reapeat in the same way its central elements (ϵ_{15}, t_{15}) so many time as to get desirable CNT channel length. Both ways of constructing system's Hamiltonian we refer to as "modular" approach. Repeating procedure should reproduce well an actual Hamiltonians of the longer systems, because either deeply inside the contact, or far from the contacts' edges all physical properties (and, thus, corresponding matrix elements of the Hamiltonian) should be the same. Which components of the CNT-metal interaction do we capture by *System* 1? – *System* 1 contains a junction between free and embedded

tube parts, which makes it possible to describe band banding felt by electron, going from the embedded tube part to the channel. Besides, **H** already contains a doping due to the metal contacts in its elements.

2. *System* 2. *System* 2 is composed of a honeycomb carbon sheet (which contains $n \times m$ supercells) on top of three slices of the metal, also composed of $n \times m$ supercells each. Boundary conditions are the same as for *System* 1. *System* 2 contains an interface between a metal and carbon, and, in contrast to *System* 1, it has sufficient metal to calculate metal's self-energy.

3. *System* 3. *System* 3 is the same as *System* 2, but it contains no carbon and no vacuum above. Together with the *System* 2 it is used to calculate a metals' self-energy.

All three systems can be built by translation of the metal's supercell and honeycomb lattice's supercell, which are shown in Fig. S11. There are several types of the supercells depending on crystalline structure of the metal and lattice constant of the metal. Number of the super-cells in the *Systems* 1,2 are also different. We can summarise this informations as follows:

(a) Au, Pd, Pt, Rh, Al – fcc lattice; direction [111]. For *Systems* 1,2, $m \times n = 3 \times 5$;

(b) Cu, Ni – fcc lattice; direction [111]. For *Systems* 1,2, $m \times n = 5 \times 9$;

(c) Sc – hcp lattice; direction [0001]. For *Systems* 1,2, $m \times n = 5 \times 3$;

(d) Ti – hcp lattice; direction [0001]. For *Systems* 1,2, $m \times n = 3 \times 5$.

Bulk DOS of the metals

As a sub-product of the self-energy calculation we have calculated bulk density of states DOS_{bulk} for 10 simulated metals (see Fig. S12). We used this plot to assure ourselves that the self-energy Σ^{Me} has been correctly calculated, because DOS_{bulk} and matrix elements of Σ^{Me} have been calculated within the same routine. These DOSes are calculated for the metallic lattices with a stress/strain included (that was introduced to fit a graphene lattice).

Hence, it proves also that we change a lattice constant of our metals not too much.
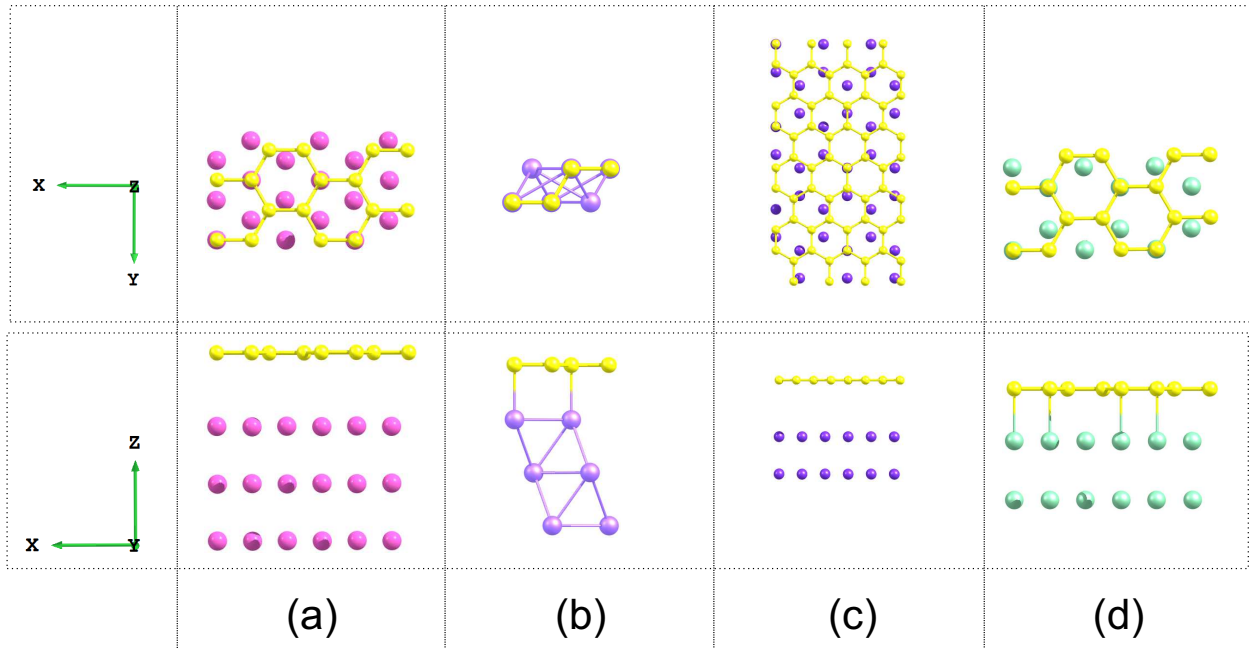

Figure S11: Top and side view of the supercells for different contact metals (upper and lower panel, respectively), shown in alignment to the corresponding supercell of the honeycomb lattice: (a) Au, Pd, Pt, Rh, Al; (b) Cu, N ; (c) Sc ; (d) Ti.
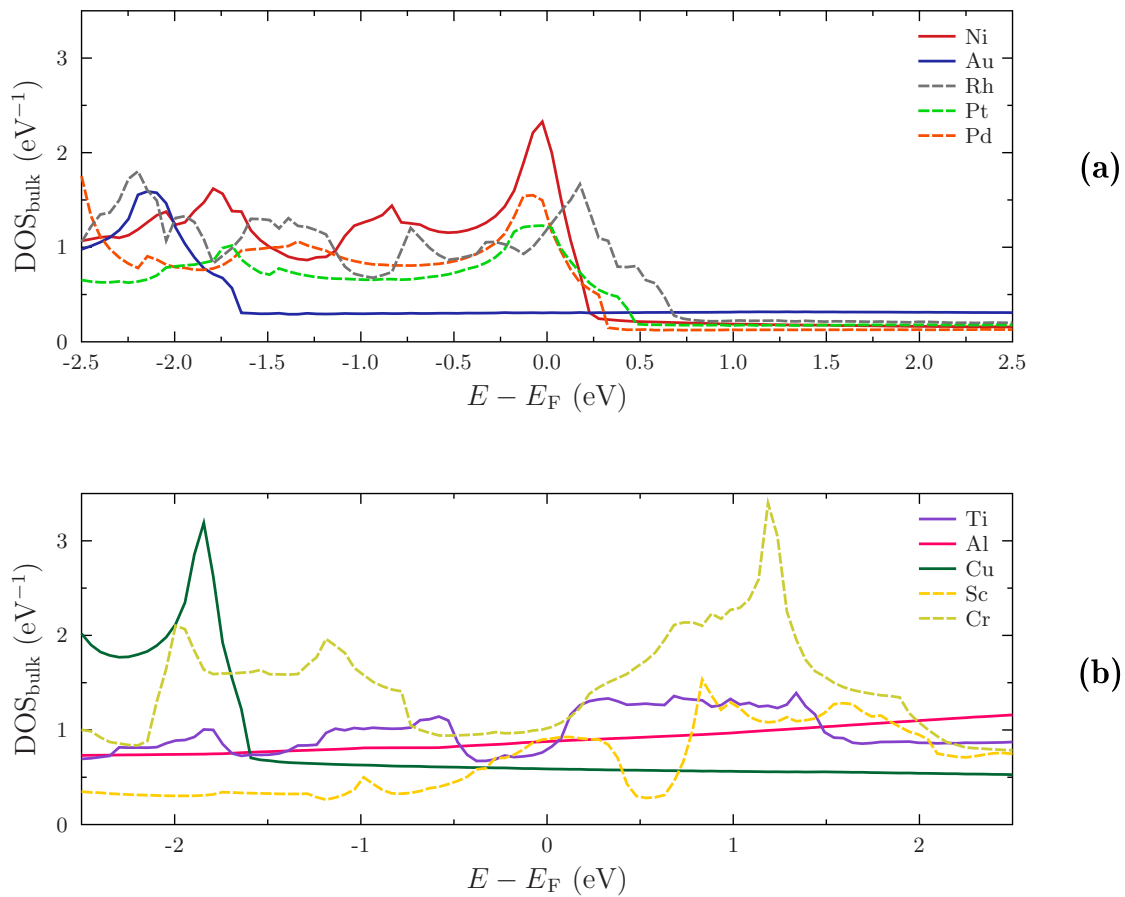
Figure S12: Bulk density of states per carbon atom for the simulated metals: (a) Ni, Au, Rh, Pt, Pd; (b) Ti, Al, Cu, Sc, Cr. All the metals are already compressed/stretched to fit a graphene lattice periodicity as shown in Fig. S11.